

Appendix F

Glare Study

This page is intentionally left blank.

GLARE STUDY

Byron Solar, LLC

Dodge and Olmstead Counties, Minnesota

JUNE 19, 2022

PREPARED FOR:



PREPARED BY:

Westwood



Glare Study

Byron Solar Project

Dodge and Olmsted Counties, Minnesota

Prepared For:
Byron Solar, LLC
10 NE 2nd Street, Suite 400
Minneapolis, MN 55413

Prepared By:
Westwood Professional Services, Inc.
12701 Whitewater Drive, Suite 300
Minnetonka, MN 55343
(952) 937-5150

Project Number: 0028109.00
Date: June 19, 2022

Executive Summary

Westwood Professional Services, Inc. (Westwood) completed a glare study using Forge Solar's GlareGauge software to analyze glare hazard for the proposed Byron Solar Project (Project) located in Dodge and Olmsted Counties, Minnesota.

Receptors modeled for glare included residences and routes within approximately 500 feet of arrays, and airport flight paths and air traffic control towers within approximately 10 miles of arrays. Seventeen residential structures were each assessed at 5-feet and 15-feet above ground level (AGL) to simulate **an observation point (OP) for person's** eye level at a first and second story for each residence (two OPs were modeled for each residence making a total of 34 OPs). Eleven public road segments (Routes) were modeled. Eight 2-mile flight paths (FP) were modeled. Four FPs from the Dodge Center Regional Airport (TOB) FP-1 through FP4, and four FPs from Rochester International Airport (RST), FP 5- FP8. Also modeled was the air traffic control tower (ATCT) at RST; it is identified as OP-5000. The location of the arrays, OPs, Routes, FPs and ATCT are shown in Exhibits 1-3.

This glare analysis used a 1.5-meter array height (AH) (rounded to 5-feet). The OPs, Routes and FPs were modeled using a 0-degree rest angle (DRA). Flight paths and the RST ATCT were also modeled using a 5-DRA to determine if glare would be reduced or eliminated.

Data are summarized in Appendix A and details are in Appendix B. The glare values of minutes/year are calculated using line of site elevations and do not account for existing vegetation or structures that would reduce the visibility of glare from arrays by physical screening. A viewshed model was also prepared for the RST ATCT to determine visibility with structures and vegetation; visibility is shown in Exhibit 4. The summary table below reports the number of residential OPs, Routes, and FP receptors receiving the three categories of glare: red glare (*potential for permanent eye damage* [retinal burn]), yellow glare (*potential for producing an after image*), and green glare (*low potential for producing an after-image*).

Number of Receptors Receiving Glare

Number of Components with Glare	Green Glare AH 5ft		Yellow Glare AH 5ft		Red Glare AH 5ft	
	0 DRA	5 DRA	0 DRA	5 DRA	0 DRA	5 DRA
Residential Observation Points (OPs)	32	NA	34	NA	0	NA
Routes	8	NA	7	NA	0	NA
Airport Flight Paths (FPs)	3	1	0	0	0	0
RST ATCT	1	1	0	0	0	0

The glare classifications in reducing severity:

- Red Glare (potential for permanent eye damage)
- Yellow Glare (potential for producing an after image)
- Green Glare (low potential for producing an after-image)
- AH (Average array height with 0 DRA)
- DRA (Degree Rest Angle of the Array)
- NA (No Analysis)

Glare with an intensity to cause permanent impacts (red glare) was not predicted in the modeled residential OPs, routes, flight paths or the ATCT.

Glare with a potential for producing an after image (yellow glare) was predicted at 34 residential OPs and 7 routes. None of the flight paths or ATCT would receive yellow glare.

Glare with a low potential for producing an after-image (green glare) was predicted at 32 residential OPs, 8 routes, 3 flight paths and the RST ATCT when modeled at 0-degrees rest angle. The FPs and ATCT were modeled at a 5-degree rest angle and one FP and the ATCT would receive glare from array 5F.

Federal Aviation Administration (FAA) requires a glare study for projects on a federally obligated airport. However, this project is not airport property. Out of due diligence, the Rochester airport air traffic control tower was modeled for glare, although the project is approximately 10 miles from the Project. This Project complies with the Federal Aviation Administration (FAA) 2021 policy because the Project is not located on a federally obligated airport.

Table of Contents

1.0	Introduction.....	5
1.1	General Discussion of Reflection	6
	Reflection Type from Solar Modules.....	6
	Relative Reflectance of Solar Modules Compared to Other Surfaces	7
1.2	Important Considerations.....	9
1.3	Overview of Sun Movements and Relative Reflections	9
	Determining the Vector Location of Incident Sunlight.....	9
1.1.1	Sunlight Geometry	10
1.1.2		
2.0	Description of the Proposed Project	11
1.3.1	2.1 Geometric Characteristics of Photovoltaic Panel Configuration and Their Influence on	
1.3.2	Perceived Glare.....	13
3.0	Identification of Observation Points, Routes, and Flight Paths	14
4.0	Glare Assessment Methodology.....	18
5.0	Glare Results	21
	5.1 Observation Points (OPs) and Route Segments.....	21
6.0	References	23

Tables

Table 1 – Location of Ops within 500 Feet of Arrays.....	15
Table 2 – Location of Routes within 500 Feet of Arrays	16
Table 3 – Location of Flight Paths from Airports within Approximately 10 Miles of the Project	17
Table 4 – Number of Receptors Receiving Glare	21

Figures

Figure 1 – Glare Hazard Plot	6
Figure 2 – Specular and Diffuse Reflections	6
Figure 3 – Light Transmission of Glass	7
Figure 4 – Analysis of Typical Material Reflectivity with Sunlight Angle	8
Figure 5 – Albedo for Various Common Surfaces	8
Figure 6 – Solar Path Chart Plotting Solar Azimuths and Elevations as a Function of Time and Date for the Location of the Proposed Solar Project	10
Figure 7 – (a) Geometry of the Reflection (L2) of an Incident Ray of Sunlight (L1) from a Vertical Reflective Surface (Source: Lillefair, 1987). (b) Reflections from a Sloping Reflective 1-Single Axis Tracker Surface (Source: Stine and Geyer, 2001)	11
Figure 8 – Diagram of the Racking System Configuration for the Proposed Project 1Mh=7.4'; 2Mh=14.8'	11
Figure 9 – Diagram Showing Tracker Array Rotation and Orientation for the Proposed Project	12
Figure 10 – Solar PV Tracker System Configuration at (a) 9:00 AM, (b) 10:00 AM, (c) 12:00 PM, and (d) 2:00 PM on December 21st, the Winter Solstice.....	12

Figure 11 – Typical 1-Axis Tracking System Configuration Elevation View A up to 2.2m @Max D;
B was assessed for 1.5m (5’); C=0.79m; D=52° to -52°; R= was assessed for 0° at all
receptors, and for flight paths and ATCT at 5° 13

Figure 12 – Residential OP Example Adjacent to Proposed Arrays..... 14

Figure 13 – Route Example..... 16

Figure 14 – Flight Path (FP) Example..... 17

Figure 15 – Air Traffic Control Tower Example 18

Figure 15 – Example of Modeled PV Sub-Array Input Parameters 19

Exhibits

- Exhibit 1: Project Site Location Map
- Exhibit 2: Project Glare Study Overview Site Map with Arrays and Receptors
- Exhibit 3: Airport Glare Study Overview Site Map with Arrays, Flight Paths, and ATCT
- Exhibit 4: Viewshed Analysis of Rochester Airport Air Traffic Control Tower

Appendices

- Appendix A: Summary Glare Data
- Appendix B: Detail Glare Data

1.0 Introduction

Westwood was contracted by Byron Solar, LLC (Byron) to prepare a glare study for the proposed Project. The study was requested by the Minnesota Department of Commerce (DOC), Energy Environmental Review and Analysis (EERA), to support the Environmental Assessment (EA) process. The towns of Kasson and Byron are nearest the Project; Kasson is approximately 1.1 miles northwest of the Project Substation and 1 mile west of the HVTL right-of-way; Byron is about 1.5 miles northeast of the Project Substation and approximately 0.2 miles south of the Proposed Route in Dodge and Olmsted Counties, Minnesota (Exhibit 1).

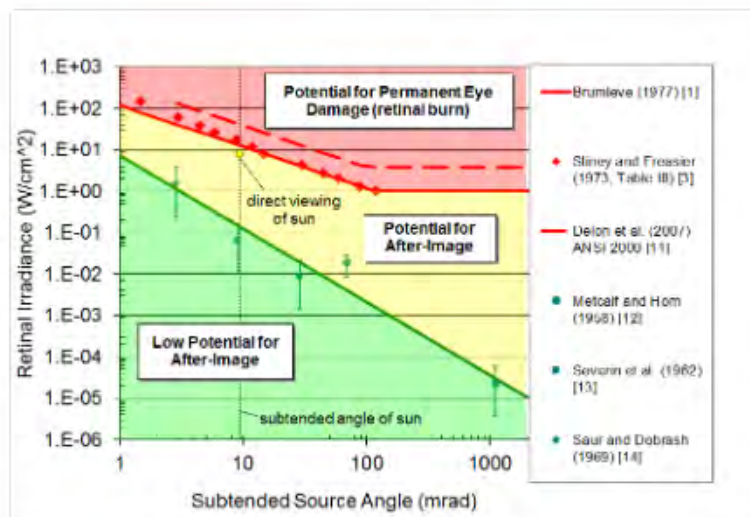
The Project will consist of a series of photovoltaic (PV) modules fixed to single axis solar trackers. Panels will be placed with participating properties and have an installed capacity of up to 200 MWAC (Exhibit 2).

Westwood used the web-based **Forge Solar's GlareGauge software to complete a glare analysis** to determine the potential for glare from the PV panels to affect pilots and airport air traffic control tower operators, residents in the area, and drivers passing through.

This study analyzes the anticipated glint and glare attributable to the Project, and any associated impact on nearby residences, roads, airport flight paths and air traffic control towers. The ocular impact (being connected to the eye or vision) of solar glare is quantified from most severe to least severe into three categories (Ho, 2011) (Figure 1):

- Red – potential to cause retinal burn (permanent eye damage)
- Yellow – potential to cause temporary after-image
- Green – low potential to cause after-image

These categories, shown in the graphic below, assume a typical blink response in the observer. Note that retinal burn is typically not possible for PV glare since PV modules do not focus reflected sunlight.



Sample glare hazard plot defining ocular impact as function of retinal irradiance and subtended source angle (Ho, 2011)

Figure 1 – Glare Hazard Plot

1.1 General Discussion of Reflection

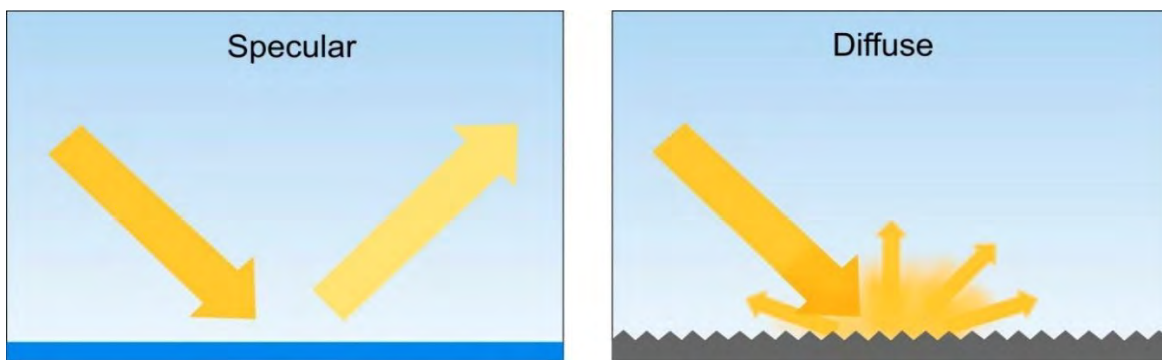
With growing numbers of solar energy facilities being proposed and installed throughout the United States, the potential impact of glare from PV modules and other types of solar collection systems is receiving increased attention as a potential nuisance to neighboring residential properties or potential hazard or distraction for vehicle drivers, pilots, and air-traffic control personnel at nearby airports.

A common misconception about solar PV modules is that they inherently cause or create a lot of glare, posing a nuisance to neighbors and a safety risk for pilots. While in certain situations the glass surfaces of solar PV modules can produce glare (a reflection of bright light for a longer duration), light absorption, rather than reflection, is central to the function of a solar PV panel. PV modules absorb solar radiation that is converted to electricity. Solar PV modules are constructed from high transmission, low iron glass and are covered with Anti-Reflective Coatings (ARC). Modern solar PV modules reflect as little as two percent of incoming sunlight, about the same as water and less than soil or even wood shingles (Sandia, 2014).

Reflection Type from Solar Modules

1.1.1

Smooth surfaces such as glass and still water exhibit specular reflection. Specular reflection is when light hits the surface at one angle and is reflected in another direction, like a mirror. Specular reflection can be contrasted with diffuse reflection, which occurs when light reflects off microscopically rough surfaces and scatters. Diffuse reflection is what happens when light hits virtually everything in our field of vision. The difference between the two types of reflections is illustrated in Figure 2. Since solar modules are flat and have a relatively smooth surface, most of the light reflected is specular, meaning that incident light from a specific direction is reradiated in a different direction.

**Figure 2 – Specular and Diffuse Reflections**

When the sun is reflected on a smooth surface, it can result in glare for those who are on the receiving angle. In both cases, the light reflected is diminished by having first hit the substrate that reflected it—unless that surface is a perfect mirror. When the sun is the original source of the light reflected off a reflective surface, the time and

position at which glare might occur depends on the original position of the sun in the sky in relation to the location of the viewer.

Relative Reflectance of Solar Modules Compared to Other Surfaces

1.1.2 Solar modules are designed to absorb light, and accordingly reflect only a small amount of the sunlight that falls on them compared to most other everyday objects. Most notably, solar modules reflect significantly less light than flat water or standard window glass. In fact, glass, one of the uppermost and important components of a solar panel, reflects only a small portion of the light that falls on it—about 2 to 4 percent, depending on whether it received an ARC. To increase solar panel efficiency and power output, most of the solar PV modules in use today are treated with an ARC. An example of how anti-reflective technology can increase light transmission in glass and reduce overall reflection is provided in Figure 3. Standard low-iron glass reflects approximately 8 percent of light, whereas ARC-glass modules reflect a total of approximately 2 to 3 percent of the light.



Figure 3 – Light Transmission of Glass

Studies have been conducted which have measured the intensity of reflections from PV solar modules with respect to other naturally occurring and manmade surfaces. The results of the studies show that reflections of the sun from solar modules are possible; however, the reflections produced will be of intensity like, or less than, those produced from still water and significantly less than reflections from glass and steel. The reflectivity of solar modules relative to other natural or manmade surfaces are provided in Figures 4 and 5.

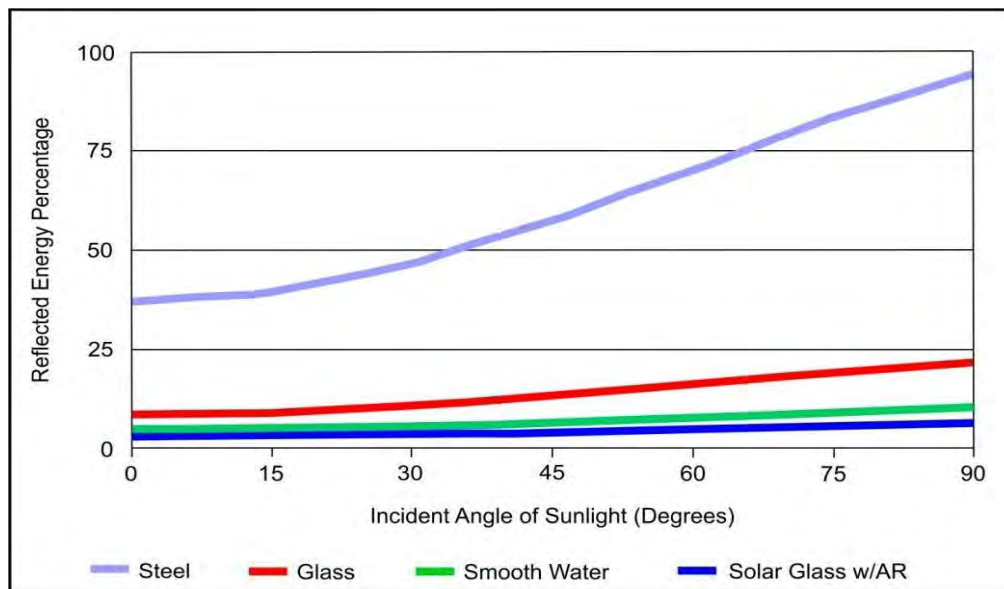


Figure 4 – Analysis of Typical Material Reflectivity with Sunlight Angle

(Source: Capital Solar Farm Visual Impact Assessment, 2010)

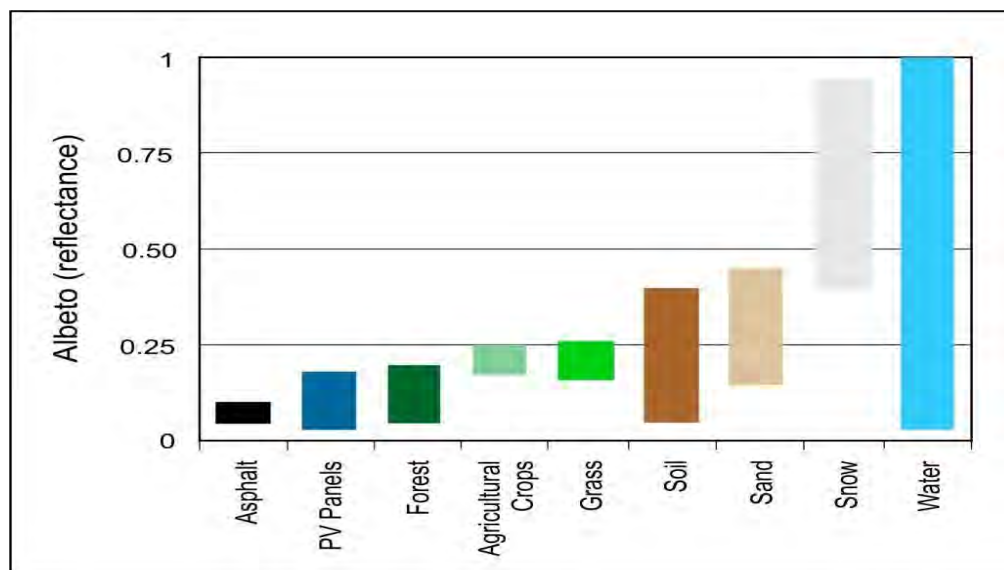


Figure 5 – Albedo for Various Common Surfaces

(Source: Capital Solar Farm Visual Impact Assessment, 2010)

One measure of reflectivity is albedo, the ratio of solar radiation across the visible and invisible light spectrum reflected by a surface. Albedo varies between 0, a surface that reflects no light, and 1, a mirror-like surface that reflects all incoming light. Solar PV modules with a single ARC have a reflectivity of between 0.03 and 0.18. Common sand has an albedo between 0.15 and 0.45 and agricultural vegetation has an albedo between 0.18 and 0.25. This diffuse reflectivity measure is consistent with the intent of solar PV modules to absorb the majority of solar energy for conversion to electricity.

1.2 Important Considerations

Before considering the mathematics of sunlight reflectivity, it is important to understand several fundamental limitations concerning the extent to which glare might be visible to nearby receptors (residences, routes, or flight paths).

First, for glare to appear, the observer must be able to see the top surface of the PV modules. For this to occur, at a minimum, the receptor would need to be at a height sufficient to slightly look down at the tops of the solar modules.

Second, since the panels will be mounted on single axis tracking systems, the surface of the panels will always try to follow the position of the sun (but fixed in one axis). Due to this property, steep glancing angles are minimized as compared to a non-tracking system.

Lastly, glare is avoided when vegetation or other impediments are located between the observer and the solar modules. A home, for example, may be in the general area of a site with solar PV modules. That house, however, is at no risk of exposure to solar glare if other buildings or trees stand between it and the solar modules.

1.3 Overview of Sun Movements and Relative Reflections

The basic concept to understand in any discussion of glare elevation is that the angle of incidence is always equal to the angle of reflectance. The empirical inquiry is then whether the potential observer is within the altitude of reflection given the distance of the observer from the solar PV panel. At any angle of reflectance, as a potential observer is further and further away from the solar PV panel, the elevation of the reflected sunlight (i.e., any glare) is more likely to be above the observer and, thus, not seen. In contrast, at a high angle of reflectance, the elevation of reflected sunlight will likely be above the observer-even at short distances.

Given the basic principle of light reflectivity, evaluating the angle of reflectance from a solar PV panel must begin with a determination of the altitude of the sun (in degrees) **relative to the ground. The “solar altitude” is the angle of the sun in degrees above or below the horizon.** As such, the most important consideration when calculating light reflectivity is not the horizon, but the angle at which the solar panel is mounted relative to the horizon.

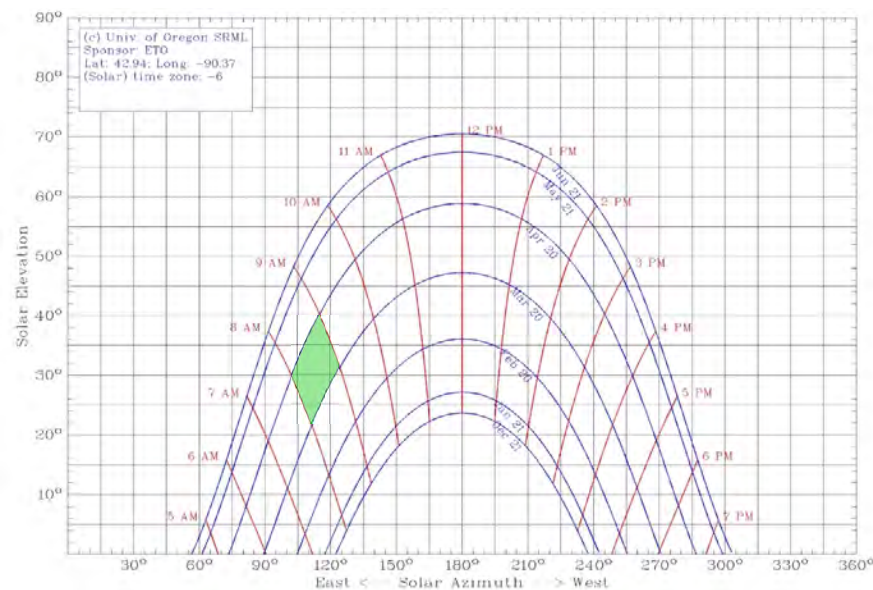
As the angle of the sun in relation to the solar PV panel increases, the angle of reflection will decrease, and the altitude of reflection will increase. The altitude of the sun differs based on a number of different factors: the time of day, the season of the year, and the latitude at which the solar PV panel is located.

Determining the Vector Location of Incident Sunlight

The sun’s apparent path across the sky changes slightly every day in known and predictable ways depending on the location of the subject area on the earth and date **of the year. At any given instant, the sun’s position in the sky can be described by a** directional vector characterized by an azimuth and an elevation. An azimuth is

defined as the angle of the sun's position from due north in a clockwise direction. For example, if the sun rose exactly in the east and set exactly in the west, the azimuth of the sunrise would be 90° from north, and the sunset would occur at 270° from the north. The sun's elevation is defined as the degrees of the sun's orb above the horizon at any instant in time. Other azimuth conventions consider azimuth from north to south along the east half as ranging from 0° to 180° , and along the west half as ranging from 0° to -180° .

Sun path chart diagrams plot the azimuth and elevation of the sun at any instant in time for any location on the earth. A sun path chart for the latitude and longitude of the proposed Project is shown in Figure 6. The sun's path for a given date is shown in blue and the time during which the sun is at a specific location in the sky is shown in red. For the location of a given receptor such as a residence, the solar elevation and azimuth where reflections would be received at the receptor can be calculated and plotted on the solar chart. For example, for the hypothetical receptor shown in green, reflected light would only be received when the sun is between approximately 75° and 90° azimuth (from north) and at an elevation between 22° and 40° . From the chart, this would occur between 8 a.m. and 9 a.m. between the dates of March 20 to April 20.



1.3.2
Figure 6 – Solar Path Chart Plotting Solar Azimuths and Elevations as a Function of Time and Date for the Location of the Proposed Solar Project

Sunlight Geometry

The determination and characterization of the geometry of incident and reflected light is a mathematical process that is based on angles and vectors in three-dimensional coordinate systems. Light reflected from a surface is described in Figure 7a & b and shows that reflected light is symmetrical about the normal of the surface. All methods used to calculate the path of reflected rays assume this symmetric condition.

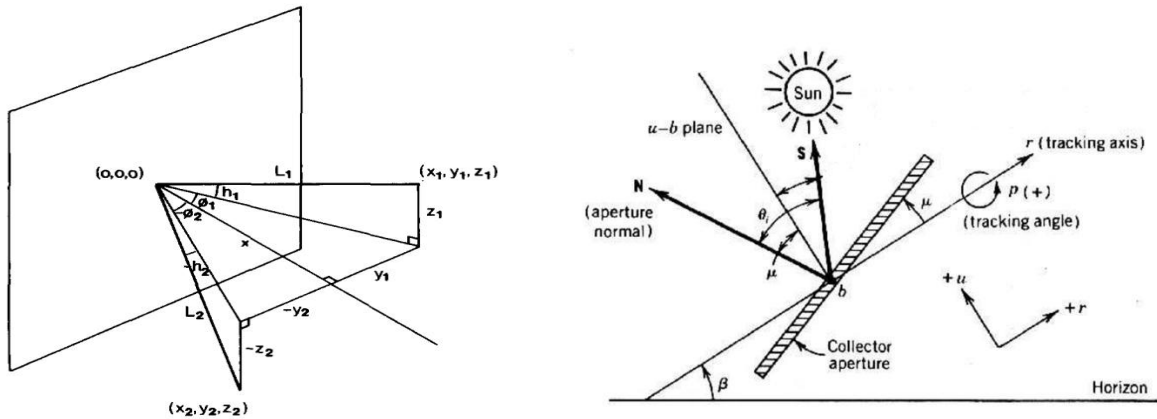


Figure 7 – (a) Geometry of the Reflection (L2) of an Incident Ray of Sunlight (L1) from a Vertical Reflective Surface (Source: Lillefair, 1987). (b) Reflections from a Sloping Reflective 1-Single Axis Tracker Surface (Source: Stine and Geyer, 2001)

2.0 Description of the Proposed Project

The Project may use PV modules from a variety of manufacturers. The modules will be divided in ranks and arranged in a series of irregular rectangular units. Modules will likely be stacked in a one or two module height (Mh) configuration in a portrait mode on a single-axis tracker system (Figure 8). The tracker will rotate east to west along a north-south axis from the horizontal in east-west oriented ranks with the panel normal oriented due south (Figures 9 and 10). When installed, dimensions of a typical single-axis tracking system elevation are shown in (Figure 11).

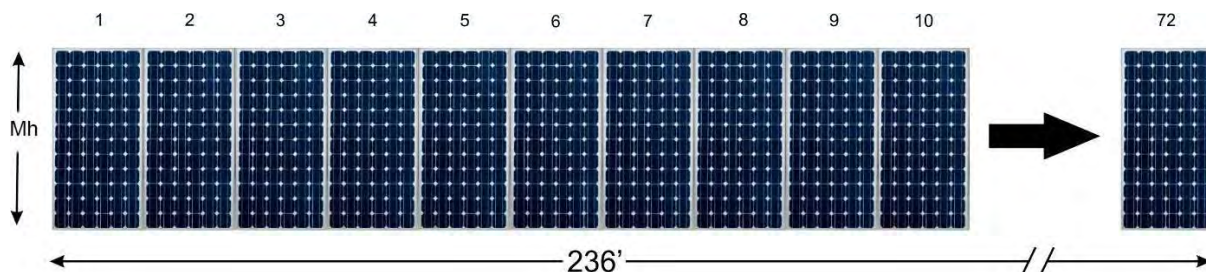


Figure 8 – Diagram of the Racking System Configuration for the Proposed Project 1Mh=7.4'; 2Mh=14.8'



Figure 9 – Diagram Showing Tracker Array Rotation and Orientation for the Proposed Project

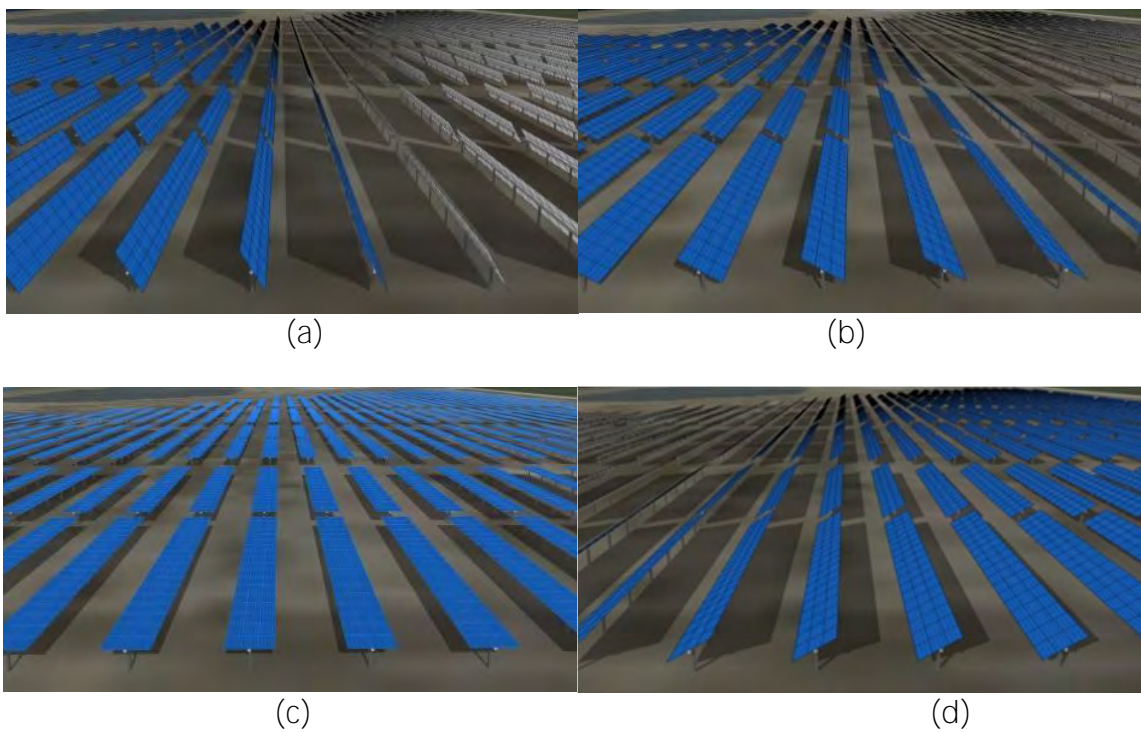


Figure 10 – Solar PV Tracker System Configuration at (a) 9:00 AM, (b) 10:00 AM, (c) 12:00 PM, and (d) 2:00 PM on December 21st, the Winter Solstice

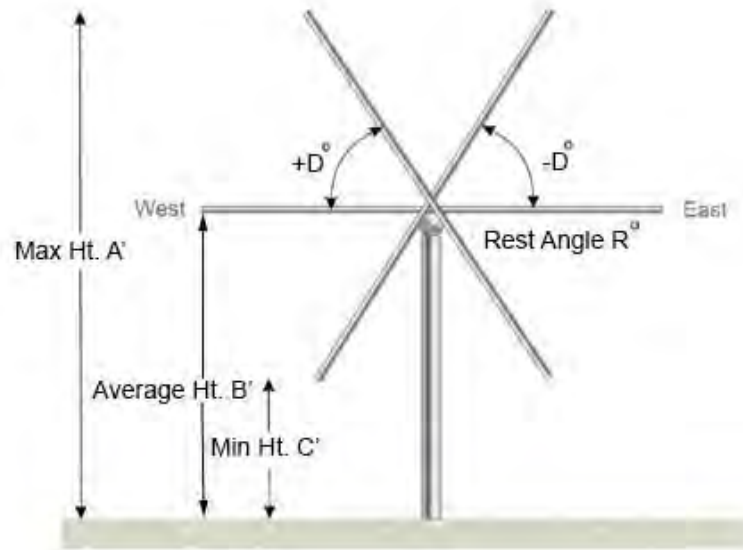


Figure 11 – Typical 1-Axis Tracking System Configuration Elevation View A up to 2.2m @Max D; B was assessed for 1.5m (5'); C=0.79m; D=52° to -52°; R= was assessed for 0° at all receptors, and for flight paths and ATCT at 5°

2.1 Geometric Characteristics of Photovoltaic Panel Configuration and Their Influence on Perceived Glare

With respect to assessing the impacts of reflected sunlight associated with PV modules for the proposed Project, the following assumptions apply:

1. Perceived glare was based on line-of-sight from the reflective surface without accounting for visual screening from vegetation or buildings.
2. The magnitude and duration of glare reflections will be related to the height of the observer. When the height of the observer is less than the module height and the landscape is flat, only one reflecting rank of PV modules will be visible at a time.
3. Stationary receptors that are below the top height of the PV modules will only see glare from those modules whose reflective surfaces are visible from that location.
The glare will move as the sun moves until the azimuth and elevation of the sun's rays are such that reflections are no longer received at the stationary receptor.
4. Because the orientation of each rank is the same, each rank will reflect glare at the same angle for the same time increment and given azimuth and elevation angle of the sun. Thus, if a car with the observer at a height below the highest point of the PV rank observes a solar reflection, the same reflection at the same relative location will be observed as the car proceeds parallel to the PV ranks.
5. As the height of the stationary receptor increases above the height of the PV rank, progressively more of the area of adjacent ranks will be observed. At low heights, the majority of the PV panel area of successive ranks is blocked, but as heights increase progressively more of the reflective area of the full array becomes contributing.

3.0 Identification of Observation Points, Routes, and Flight Paths

Seventeen residences modeled at two heights each account for thirty-four residential OPs 1000-1034; an example is shown in Figure 12. These residences are located within approximately 500 feet of the proposed arrays and were assessed at 5 feet and 15 feet AGL to simulate eye level at a first and second story for each residence (2 OPs for each residence). OPs were selected within 500 feet of arrays because the lowest possible reflection angle off PV panels is 4 degrees above horizon (see panel behavior in Figures 7a and 7b, 9, 10 and 11), at 500 feet from solar PV arrays, reflections are 35 feet above the arrays when at the same elevation. Therefore, locations farther from these sites will be less likely to receive glare impacts if the elevation is at or lower than the arrays. The first-floor receptor of a residence was assigned an even identification (ID) number and the second floor of that OP was assigned the next odd ID number. For example: OP 1000 and OP 1001 are the same residence at the first and second floor levels.



Figure 12 – Residential OP Example Adjacent to Proposed Arrays

Specific details regarding the OPs Modeled in relation to the solar arrays are presented in Table 1, and the locations of the OPs and PV arrays are depicted in Exhibit 2.

Table 1 – Location of Ops within 500 Feet of Arrays

Glare ID	OP ID	Latitude	Longitude	Elevation (ft)	OP Height (ft)	OP Elev (ft)
1000	1	44.016465	-92.697019	1264.019069	5	1269.019069
1001	1	44.016465	-92.697019	1264.019069	15	1279.019069
1002	2	44.007901	-92.702163	1274.852403	5	1279.852403
1003	2	44.007901	-92.702163	1274.852403	15	1289.852403
1004	3	44.008101	-92.724175	1310.672614	5	1315.672614
1005	3	44.008101	-92.724175	1310.672614	15	1325.672614
1006	4	44.000833	-92.723495	1313.294005	5	1318.294005
1007	4	44.000833	-92.723495	1313.294005	15	1328.294005
1008	5	44.000166	-92.723123	1310.469202	5	1315.469202
1009	5	44.000166	-92.723123	1310.469202	15	1325.469202
1010	6	43.999558	-92.720416	1290.876026	5	1295.876026
1011	6	43.999558	-92.720416	1290.876026	15	1305.876026
1012	7	44.000131	-92.7176	1275.954765	5	1280.954765
1013	7	44.000131	-92.7176	1275.954765	15	1290.954765
1014	8	44.000787	-92.705892	1264.819594	5	1269.819594
1015	8	44.000787	-92.705892	1264.819594	15	1279.819594
1016	9	44.00004	-92.705319	1262.208046	5	1267.208046
1017	9	44.00004	-92.705319	1262.208046	15	1277.208046
1018	10	43.992564	-92.698537	1240.39046	5	1245.39046
1019	10	43.992564	-92.698537	1240.39046	15	1255.39046
1020	11	43.991874	-92.699157	1235.577467	5	1240.577467
1021	11	43.991874	-92.699157	1235.577467	15	1250.577467
1022	12	43.99231	-92.689913	1191.771692	5	1196.771692
1023	12	43.99231	-92.689913	1191.771692	15	1206.771692
1024	13	43.989367	-92.696776	1211.850432	5	1216.850432
1025	13	43.989367	-92.696776	1211.850432	15	1226.850432
1026	14	43.985495	-92.676915	1178.441639	5	1183.441639
1027	14	43.985495	-92.676915	1178.441639	15	1193.441639
1028	15	43.980229	-92.697137	1222.536128	5	1227.536128
1029	15	43.980229	-92.697137	1222.536128	15	1237.536128
1030	16	43.979025	-92.688464	1227.440984	5	1232.440984
1031	16	43.979025	-92.688464	1227.440984	15	1242.440984
1032	17	43.977785	-92.686378	1216.676548	5	1221.676548
1033	17	43.977785	-92.686378	1216.676548	15	1231.676548

Nine public road segments within 500 feet of the arrays were also assessed for glare. An example of 255th St is shown in Figure 13. Specific details regarding the Routes modeled for glare are presented in Table 2. The routes were assessed for glare using a height of 3.5 feet AGL to simulate an average eye level of a driver of a passenger vehicle following Federal Highway Administration Guidance (US Department of Transportation, 2022). A maximum separation

distance between the route and nearest array of 500-feet was selected because the minimum glare reflection would be at least 35 feet above the arrays. This would accommodate elevation changes such as hills and valley along a route in this relatively flat area.

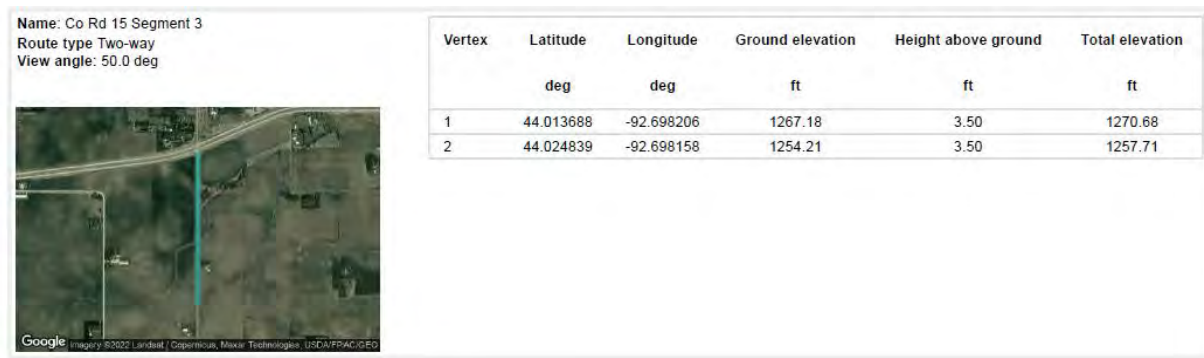


Figure 13 – Route Example

Table 2 – Location of Routes within 500 Feet of Arrays

Label ID	Route Name	Latitude	Longitude	Ground Elevation (ft)	Eye Height (ft) Above Ground
10000	Co Rd 6	43.9788	-92.6984	1210.2	3.5
10004	Co Rd 8	43.97867	-92.6783	1236.9	3.5
10010	Co Rd 15 Segment 1	43.97841	-92.6982	1211.732	3.5
10008	Co Rd 15 Segment 2	43.99218	-92.6982	1235.8	3.5
10020	Co Rd 15 Segment 3	44.01369	-92.6982	1267.1	3.5
10012	262 Ave	43.9905	-92.7133	1254.1	3.5
10014	655th St	44.00037	-92.7012	1249.0	3.5
10016	650th St	44.007741	-92.72409	1310.5	3.5
10018	265th Ave	44.00762	-92.7083	1288.7	3.5
10022	US Hwy 14 Segment 1	44.02491	-92.6994	1259.1	3.5
10027	US Hwy 14 Segment 2	44.02459	-92.7037	1269.3	3.5
10030	660th St	43.99336	-92.6982	1237.3	3.5

Eight flight paths and one ATCT were the aviation features assessed for glare from two airports within approximately 10 miles of the Project. Dodge Center Regional Airport (TOB) is located northwest of the project and has FP-1 through FP-4 (Exhibit 3). Rochester International Airport (RST) is located southeast of the project and has FP-5- FP-8. Details regarding the FPs modeled for glare are presented in Table 3. An example is shown in Figure 14. The Rochester ATCT is identified as OP-5000. Details of the ATCT modeled for glare are shown in Figure 15.

2-Mile Flight Path Receptor(s)

Name: FP 1 TOB 340
 Description: None
 Threshold height : 50 ft
 Direction: 340.0 deg
 Glide slope: 3.0 deg
 Pilot view restricted? Yes
 Vertical view restriction: 30.0 deg
 Azimuthal view restriction: 50.0 deg

Point	Latitude	Longitude	Ground elevation	Height above ground	Total elevation
	deg	deg	ft	ft	ft
Threshold	44.012052	-92.828673	1301.36	50.00	1351.37
2-mile point	43.984069	-92.818548	1301.76	603.03	1904.79



Figure 14 – Flight Path (FP) Example

Table 3 – Location of Flight Paths from Airports within Approximately 10 Miles of the Project

Dodge Center Municipal Airport (TOB)							
Direction	Flight Path	Vertex/ID	Lat (deg)	Long (deg)	Elevation	HaG Ft	Tot. Elev.
340	FP 1	1	44.012052	-92.828673	1301.3	50	1351.3
	FP 1	2	43.984069	-92.818548	1301.7	603	1904.7
160	FP 2	1	44.022362	-92.832343	1297.7	50	1347.7
	FP 2	2	44.050438	-92.841959	1230.1	671	1901.1
220	FP 3	1	44.021787	-92.830713	1294.6	50	1344.6
	FP 3	2	44.042547	-92.802694	1247.2	650.8	1898.1
40	FP 4	1	44.017629	-92.836311	1290.9	50	1340.9
	FP 4	2	43.997217	-92.864818	1297.4	596.9	1894.3

Rochester International Airport (RST)							
Direction	Flight Path	Vertex/ID	Lat (deg)	Long (deg)	Elevation	HaG Ft	Tot. Elev.
130	FP 5	1	43.919222	-92.5107	1270.3	50	1320.3
	FP 5	2	43.938882	-92.540167	1223.7	650	1873.7
310	FP 6	1	43.904537	-92.48832	1301.6	50	1351.6
	FP 6	2	43.885783	-92.457743	1272.2	632.8	1905
20	FP 7	1	43.895715	-92.506386	1314.8	50	1364.8
	FP 7	2	43.869933	-92.524566	1257.7	660.5	1918.2
200	FP 8	1	43.912055	-92.495162	1284.1	50	1334.1
	FP 8	2	43.937761	-92.476771	1230.2	657.3	1887.5

Discrete Observation Receptors

Number	Latitude	Longitude	Ground elevation	Height above ground	Total Elevation
	deg	deg	ft	ft	ft
5000-ATCT	43.911450	-92.492299	1291.06	70.00	1361.07

5000-ATCT map image



Figure 15 – Air Traffic Control Tower Example

4.0 Glare Assessment Methodology

For more detailed glare modeling results, the Project was divided into smaller sub-arrays as shown in Exhibit 2. To model the potential intensity and time of project-related glare to **receptors**, Westwood used Forge Solar’s GlareGauge solar glare analysis software (formally the Solar Glare Hazard Analysis Tool [SGHAT]). GlareGauge is a web-based tool that estimates when and where solar glare could occur throughout a typical year from a PV array as viewed from specified observer locations. GlareGauge uses an interactive ArcMap or Google Map interface together with a few user-specified parameters such as orientation and tilt of the modules to quickly locate a site, outline the proposed array, and calculate the occurrence, intensity, and size of the potential glare throughout the year.

When glare potential is predicted, the GlareGauge calculates the retinal irradiance and subtended angle (size/distance) of the glare source to estimate potential ocular hazards. Ocular hazards range in severity from a potential temporary after-image to retinal burn. GlareGauge produces a color-coded display of the potential for glare to result in an ocular impact. The glare classifications are low potential for producing an after-image (green), potential for producing an after image (yellow), and potential for permanent eye damage (red).

After the Project Area is determined and its design characteristics are known, information from each glare-sensitive receptor is input into the model. Each of the OPs were identified on the project map as an OP and the height of the observer was incorporated. Each OP was assessed with a solar panel resting angle of 0-degrees; airport flight paths were also modeled at 5-degrees since the receptors are higher. An example of the GlareGauge model is shown in Figure 15.

The FAA issued guidance in 2013 regarding glare assessment for PV solar projects on and near airports. The Forge Solar site provides an evaluation of adherence to this policy which determines if yellow glare is predicted along flight paths or any glare at air traffic control towers. This guidance was superseded by FAA in 2021 final guidelines. The FAA published a final policy aimed at ensuring that airport solar projects do not create hazardous glare. The policy requires airports to measure the visual impact of such projects on pilots and air traffic control personnel.

The policy applies to proposed solar energy systems at federally obligated airports with control towers. Federally obligated airports are public airports that have accepted federal assistance in the form of grants of property conveyances. This project is not located on airport property.

As more airports invest in this technology for environmental and economic benefits, the FAA **wants to make sure that the reflection from the systems' glass surfaces do** not create a glare that poses a safety hazard for pilots and air traffic controllers.

Under the final policy, airports are no longer required to submit the results of an ocular analysis to FAA. Instead, the airport must file a Notice of Proposed Construction or Alteration Form 7460-1 that includes a statement that the project will not cause any visual impact. The airport submits the form to the FAA for review and approval (FAA, 2021).

PV Array(s)

Total PV footprint area: 206.9 acres

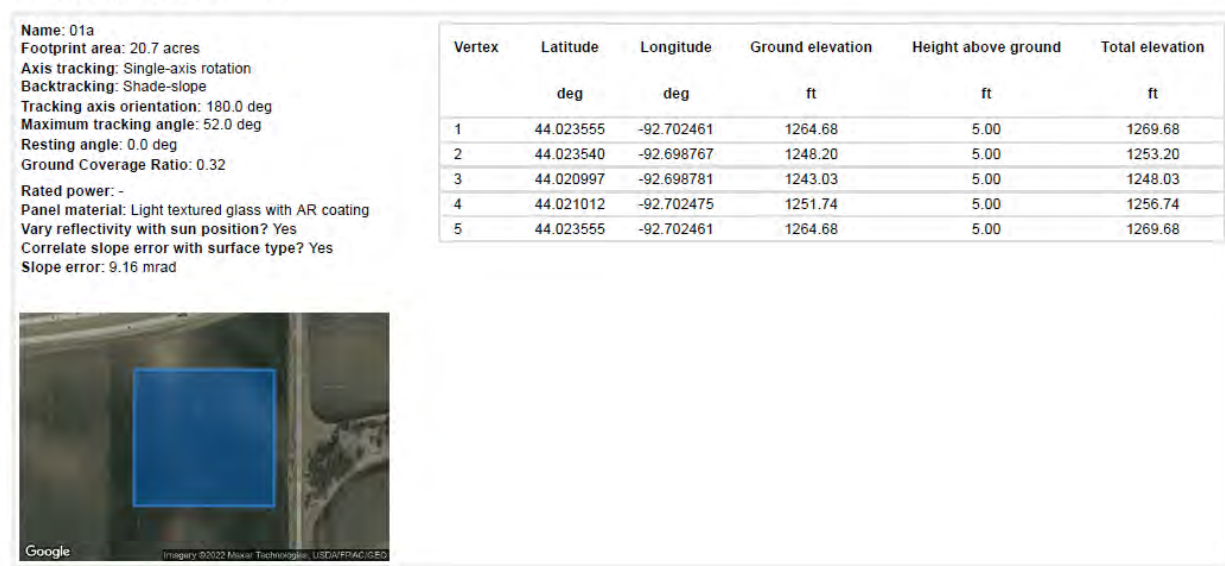


Figure 15 – Example of Modeled PV Sub-Array Input Parameters

Tilt of Tracking Axis – Elevation angle of the tracking axis in degrees, where 0° is facing skyward and 90° is facing horizontally. The modules rotate about the tracking axis. 0° was selected as the modules will be facing up.

Orientation of Tracking Axis – Orientation of the tracking axis in degrees, measured clockwise from true north. In this case the value was determined to be 180°.

Offset angle of Module – The vertical offset angle between the tracking axis and the panel. No offset was selected for the single axis tracker.

Maximum Tracking Angle – The maximum angle the panel will rotate in both the clockwise and counterclockwise directions from the zenith (upward) position.

Rated Power (kW) – kW power of solar PV plant. No rated power was selected for the proposed size of the solar arrays because the area of panel coverage is the primary factor at this site.

Module Surface Material – Type of PV material used and surface finish of panel. According to specifications from the module manufacturers, it was determined that the input ‘Smooth Glass with ARC’ would be the most representative option.

Reflectivity of PV Module – The near-normal specular reflectance of PV glass (e.g., with ARC) can be as low as 2%, the reflectance can increase as the incidence angle of the sunlight increases (glancing angles). This number is based in part on the array parameters shown in Figure 12.

Slope Error – Mirror-like surfaces that produce specular reflections will have a slope error closer to zero, while rough surfaces that produce more scattered (diffuse) reflections have higher slope errors. Based on typical values for the module types under consideration, an 8.43 mrad (slope error limit) was used.

Latitude and Longitude – The latitude and longitude of the PV array boundary vertices were used to define the area covered by proposed PV array. Appendix A provides the coordinates of the perimeter and their map image which also correspond to PV arrays shown in Exhibit 2. GlareGauge creates a reflective plane using elevation values of the array for the glare assessment.

Ground Elevation – Elevation of vertices above sea level. Values are input into the table once the vertex is located. This is considered the point’s base elevation. This value is used to shape the reflective plane used to estimate glare.

Height above Ground – User input to modify/correct vertex elevation above ground. This is defined as ‘PV array installation height above ground.’ Since this Project will use a single axis tracker system the height varies as shown in Figure 10.

Total Elevation – Calculated after adding the ‘Ground Elevation’ and “Height above Ground.’ All units are in feet.

Observation Point Parameters

OP parameters were receptor points located using GIS software and aerial photographs of the Project. Location, elevation, and a calculated field of the receptors were used. For residences, a 5-foot height above ground was used for first floor receptor height. A 15-foot height above ground was used for second floor receptor height (Appendix A). For the ATCT the published height of the tower above ground was used.

Flight Path (FP) Parameters

Flight paths are straight line landing patterns into the airport. FP parameters were calculated using GIS software and aerial photographs of the Project. Location, elevation, and a calculated field of receptors were used. A 50-foot threshold height at the airport and 3-degree glide path above ground was used for receptor height. These parameter units are in feet (Appendix A).

Total Elevation – Is calculated after adding the ‘Ground Elevation’ and ‘Height above Ground’ (HaG). All units are in feet.

Ground Elevation – Elevation of OPs above sea level. Values are pulled into the table once the OP is located. This is the point’s base elevation.

Eye level Height above Ground – User input to modify/correct observer’s elevation above ground.

5.0 Glare Results

5.1 Observation Points (OPs) and Route Segments

Results from the GlareGauge analysis determined that glare occurred most at the OPs, FPs, and Routes when the array rest angle was 0 degrees for all components and additionally at 5 degrees for flight paths and the ATCT. Glare is most frequently predicted just after sunrise, when the sun is low on the horizon and viewers are looking east at the arrays, and just before sunset, when the sun is low on the horizon and viewers are looking west at the arrays. This is summarized in Appendix A and model output details are in Appendix B.

Table 4 shows the number of receptors receiving glare when the array has a 0-degree rest angle, and for flight paths and the ATCT when the array has a 0-degree and 5-degree rest angle. No red glare is predicted from the arrays modeled at the OPs, routes, flight paths or ATCT.

Yellow glare is predicted to OPs and routes.

Green glare is predicted at OPs routes flight paths and the ATCT. It is predicted from array 5F for one flight paths and at the ATCT if a 5-degree rest angle is used.

The Project is also in compliance with the 2021 FAA guidance for glare because this Project is not located on a federally obligated airport.

Table 4 – Number of Receptors Receiving Glare

Number of Components with Glare	Green Glare AH 5ft		Yellow Glare AH 5ft		Red Glare AH 5ft	
	0 DRA	5 DRA	0 DRA	5 DRA	0 DRA	5 DRA
Residential Observation Points (OPs)	32	NA	34	NA	0	NA
Routes	8	NA	7	NA	0	NA
Airport Flight Paths (FPs)	3	1	0	0	0	0
RST ATCT	1	1	0	0	0	0

The glare classifications in reducing severity:

Red Glare (potential for permanent eye damage)

Yellow Glare (potential for producing an after image)

Green Glare (low potential for producing an after-image)

AH (Average array height with 0 DRA)

DRA (Degree Rest Angle of the Array)

NA (No Analysis)

For glare models, glare is calculated using line of site elevations; the model does not account for existing vegetation or structures. This reports a worst case for glare. The viewshed analysis was only completed to determine if vegetation or structures obscured the ATCT at Rochester airport

(Exhibit 4). Portions of the arrays are predicted to be visible from the ATCT. It does not mean that being visible would result in glare being produced or visible. Arrays can be visible yet not produce glare at a given receptor.

When an array resting angle is more than 0 degrees, as an observer is further away from the array, the elevation of the reflected sunlight (i.e., glare) is more likely to be reflected above the observer and thus, not seen. In contrast, at a high angle of reflectance, the elevation of reflected sunlight will likely be above the observer, even at short distances. As the angle of the sun in relation to the solar PV panel increases, the angle of reflection will decrease, and the altitude of reflection will increase. Due to minimum elevation changes between OPs and the angle of the sun in relation to the solar PV arrays, glare will occur at lower elevations during the spring and fall equinox to the west and south of the Project during morning hours, and during the winter solstice in the east during evening hours.

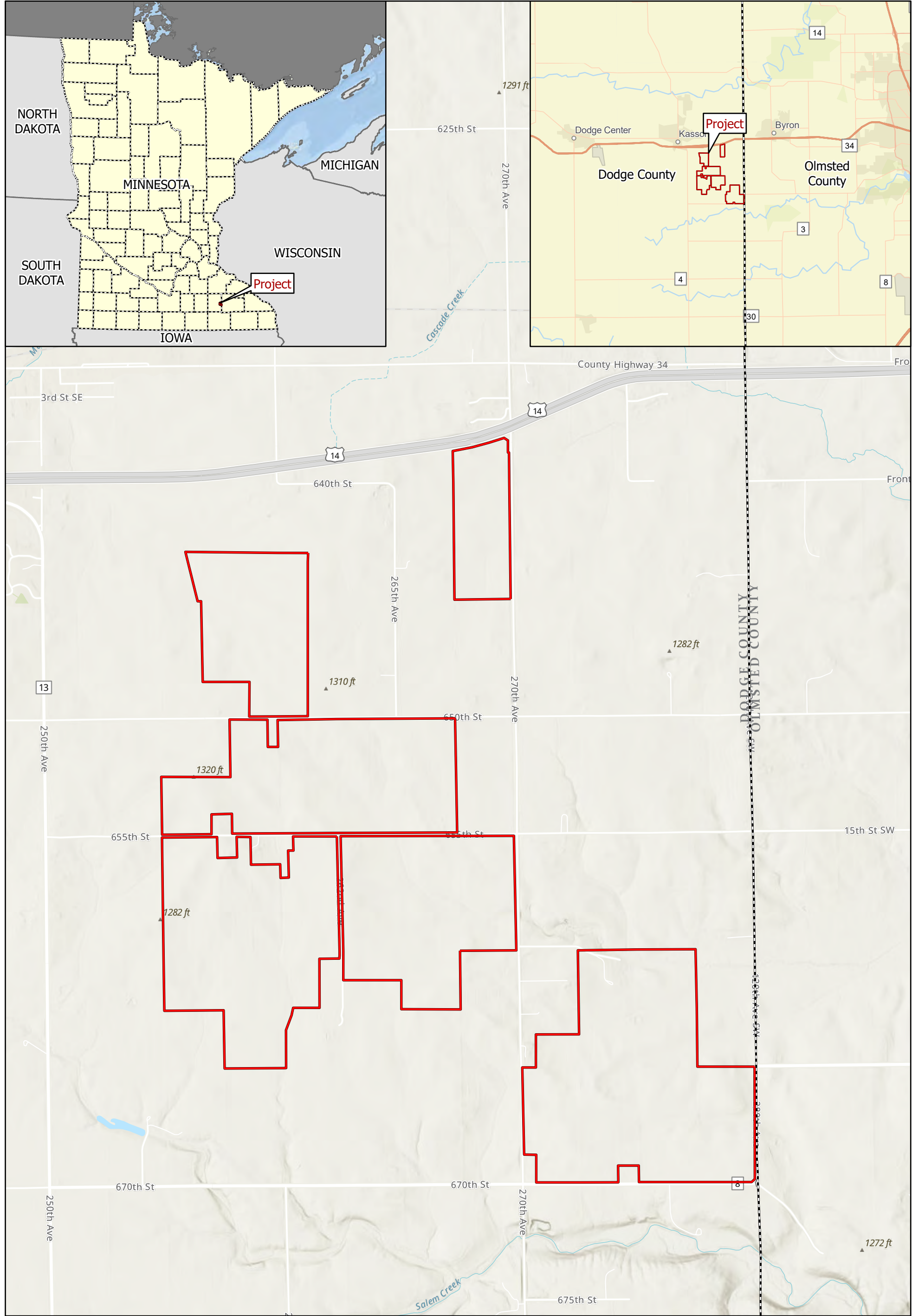
No red glare was predicted for the project. Yellow glare is predicted at 34 OPs and 7 route segments with a 0-DRA. Green glare is predicted at 32 OPs at a 0-DRA, 8 route segments, 3 flight paths, and the Rochester ATCT from up to 15 sub-arrays.

Flight paths and the ATCT were also modeled using a 5-DRA; predicted glare is significantly less with this rest angle. Red or yellow glare is predicted using 5-DRA. One FP and the ATCT were predicted to receive green glare from one sub-array using a 5-DRA. Summaries and details are shown in Appendix A and B, respectively.

6.0 References

- Capital Solar Farm Visual Impact Assessment. 2010. Available at https://majorprojects.affinitylive.com/public/a56f5113529f7061acb6de0cb400a52e/Capital%20EA%20Final%201.0%20Appendix%20F_compressed-Part4%20.pdf
- FAA. (2021, May 26). *faa-issues-policy-solar-projects-airports*. Retrieved from United States Department of Transportation, Federal Aviation Administration: <https://www.faa.gov/newsroom/faa-issues-policy-solar-projects-airports>
- Ho, C. K., Ghanbari, C. M., and Diver, R. B., 2011, "Methodology to Assess Potential Glint and Glare Hazards From Concentrating Solar Power Plants: Analytical Models and Experimental Validation", *ASME J. Sol. Energy Eng.*, 133. [\(Download\)](#)
- Lillefair, P.D. 1987. Prediction of reflected solar dazzle from sloping facades. *Building and environment* 22(4):285-291).
- Sandia National Laboratories (Sandia). 2014. Solar Glare Hazard Analysis Tool (SGHAT) **User's Manual, Ver 2D. Sandia National Laboratories. 34 pp.**
- Stine, W.B. and M. Geyer. 2001. Power from the Sun. e-book Power from the Sun.net.
- US Department of Transportation, F. H. (2022, 05 04). *5.1.4 Recommended Guidelines - FHWA*. Retrieved from [mutcd.fhwa.dot.gov](https://mutcd.fhwa.dot.gov/rpt/tcstoll/chapter514.htm): <https://mutcd.fhwa.dot.gov/rpt/tcstoll/chapter514.htm>

Exhibits

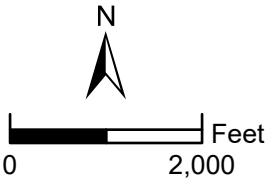


Data Source(s): Westwood (2022); ESRI WMS World Streets Basemap and Topographic Basemaps (Accessed 2021); U.S. Census Bureau (2020).

Westwood

Toll Free (888) 937-5150 westwoodps.com
Westwood Professional Services, Inc.

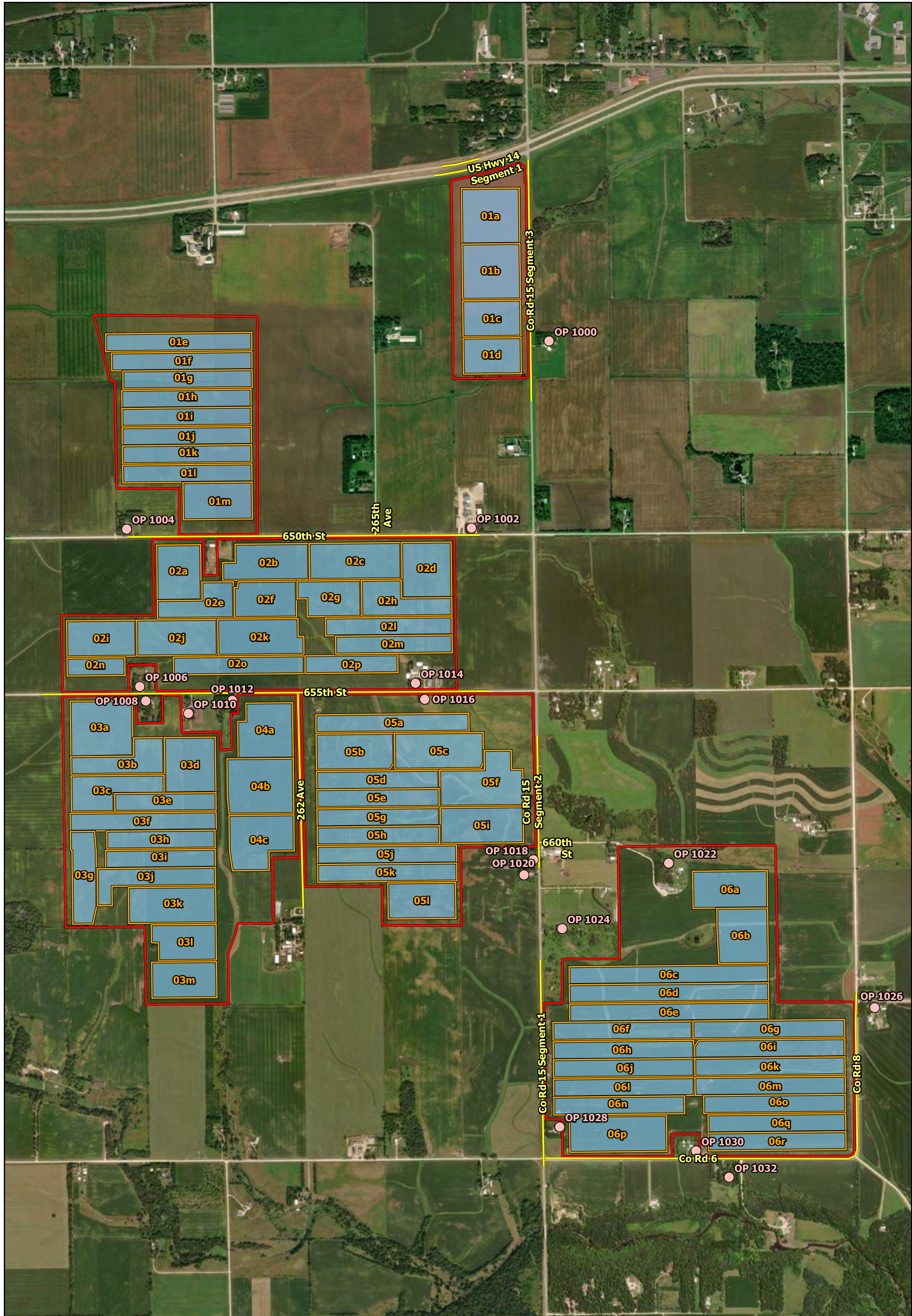
- Legend**
- Project Area
 - County Boundary
 - State Boundary



Byron Solar Project
Dodge County, Minnesota

Site Location

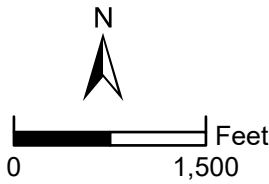
EXHIBIT 1



Data Source(s): Westwood (2022); NAIIP (2019); U.S. Census Bureau (2020).

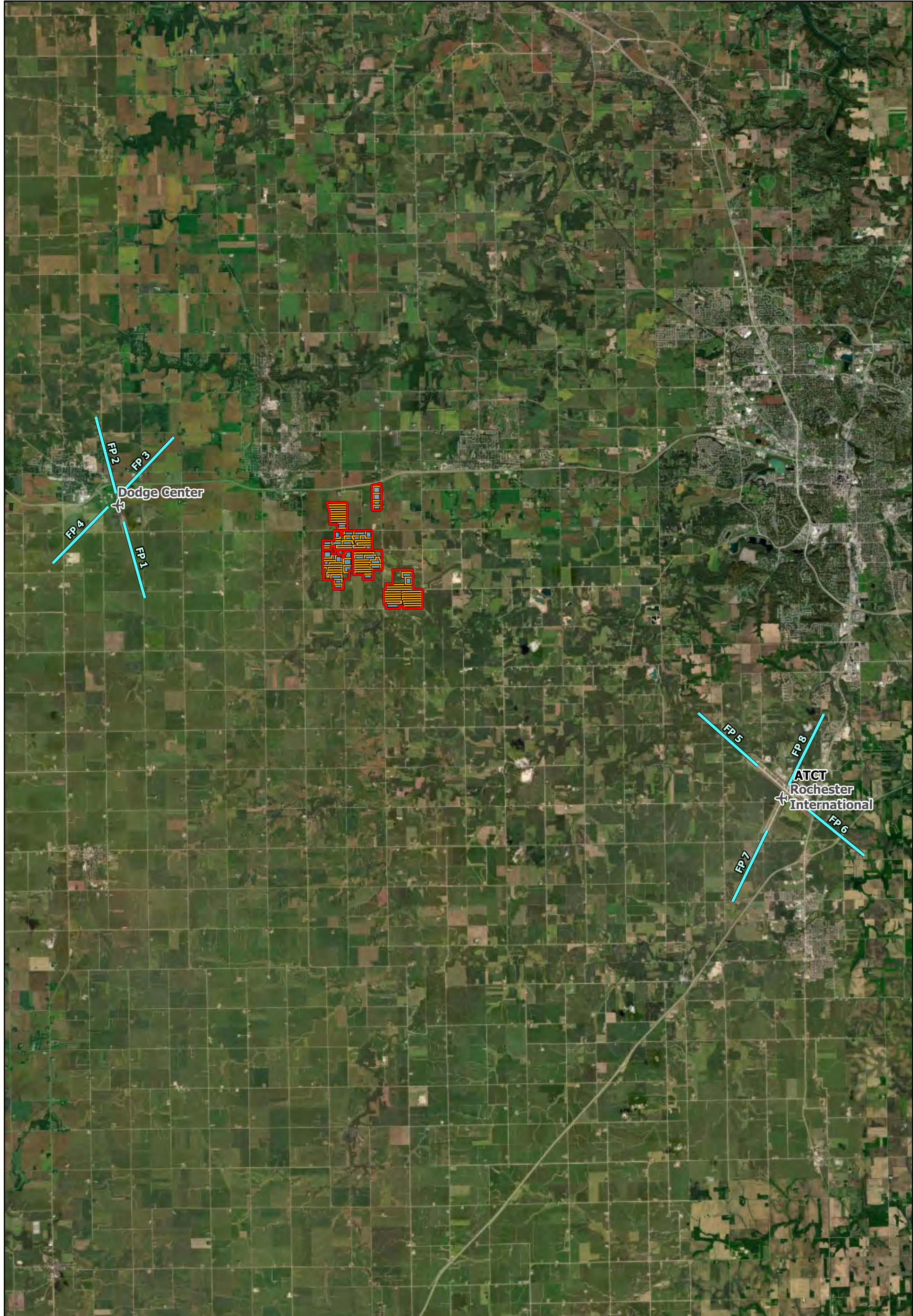
Legend

- Project Area
- Solar Array Group
- Road Receptor
- Residence Receptor (OP)



Byron Solar Project
Dodge County, Minnesota

Glare Study Overview



Data Source(s): Westwood (2022); NAIP (2019); U.S. Census Bureau (2020).

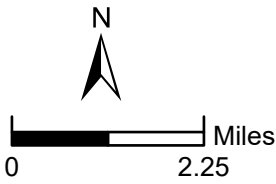
- Legend**
- Project Area

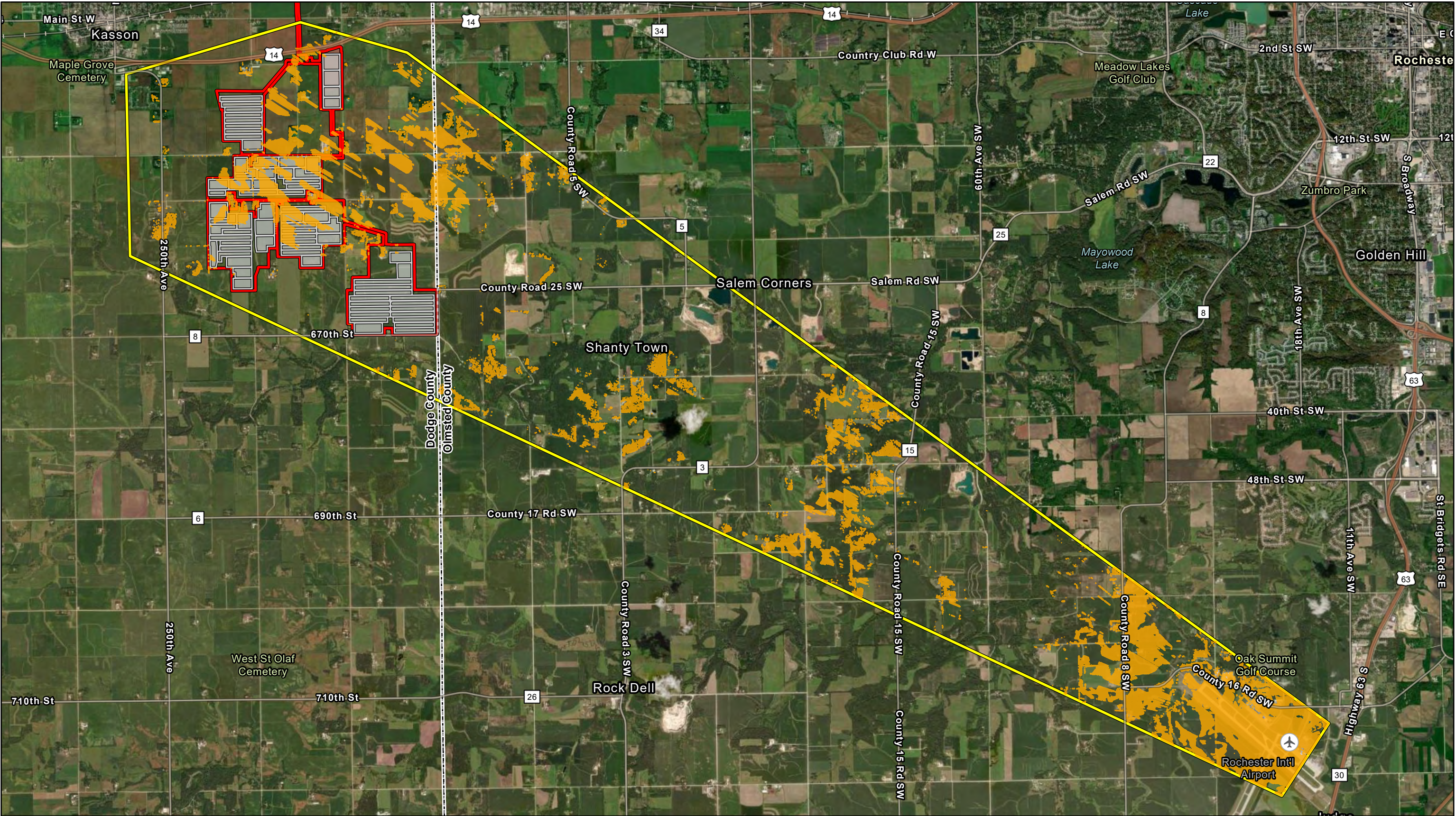
Solar Array Group

Control Tower

Flight Path (FP)





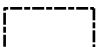

Airport



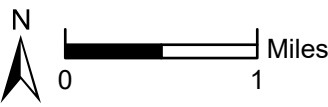


Data Source(s): Westwood (2022); ESRI WMS Hybrid World Imagery Basemap (Accessed 2022); MN Topo (2022).

Legend

- | | |
|---|--|
|  Project Area Boundary |  Rochester International Airport Air Traffic Control Tower Location (Viewshed Observer) |
|  Solar Array Group |  Area of Visibility |
|  County Boundary |  Viewshed Analysis Area |

Westwood
Toll Free (888) 937-5150 westwoodps.com
Westwood Professional Services, Inc.



Byron Solar Project
Dodge & Olmsted Counties, Minnesota

Viewshed Analysis Map

EXHIBIT 4

Appendix A

Summary Glare Data

Appendix A
oDRA
Summary Glare
Data

Array 2 with 0 Degree Rest Angle Green Glare Min/Yr																	
Component	02a	02b	02c	02d	02e	02f	02g	02h	02i	02j	02k	02l	02m	02n	02o	02p	Maximum Minutes
OP 1002	-	275	-	-	9	-	-	-	-	532	1077	-	-	-	721	290	1077
OP 1003	-	292	12	-	400	6	-	-	-	536	1100	-	-	-	767	312	1100
OP 1004	-	-	-	-	-	-	-	-	-	-	-	-	36	-	102	12	102
OP 1005	-	-	42	-	-	-	-	-	-	-	-	-	48	-	107	18	107
OP 1006	-	5	333	-	16	342	838	-	-	-	-	312	205	-	2	-	838
OP 1007	-	5	374	-	17	349	860	-	-	-	-	322	215	-	2	-	860
OP 1008	-	-	290	-	-	353	790	-	-	-	-	422	260	19	-	-	790
OP 1009	-	-	327	-	-	352	822	-	-	-	-	450	274	16	1	-	822
OP 1010	-	-	1	-	-	-	542	-	-	-	-	729	440	-	-	-	729
OP 1011	-	-	151	-	-	-	559	-	-	-	-	737	455	-	-	-	737
OP 1012	-	-	-	-	-	-	200	-	-	-	-	474	349	-	-	-	474
OP 1013	-	-	-	-	-	-	201	-	-	-	-	476	362	-	-	-	476
OP 1014	-	533	-	-	1224	245	63	-	-	499	43	-	-	-	-	-	1224
OP 1015	-	556	-	-	1102	405	63	-	-	499	42	-	-	-	81	2	1102
OP 1016	-	426	-	-	1156	387	-	-	-	570	189	26	1	-	-	-	1156
OP 1017	-	396	-	-	1210	620	-	-	-	622	192	32	1	-	1	45	1210
Route: 262 Ave	-	-	-	-	-	-	-	-	-	-	-	-	-	-	-	-	0
Route: 265th Ave	-	-	-	-	-	-	-	-	-	-	-	-	-	-	20	-	20
Route: 650th St	-	702	-	-	844	500	940	-	13	767	394	436	214	3	898	243	940

Array 2 with 0 Degree Rest Angle Yellow Glare Min/Yr																	
Component	02a	02b	02c	02d	02e	02f	02g	02h	02i	02j	02k	02l	02m	02n	02o	02p	Maximum Minutes
OP 1002	-	270	-	1066	-	-	-	134	-	-	111	-	-	-	-	-	1066
OP 1003	-	309	548	1353	-	-	-	386	-	-	137	-	-	-	-	-	1353
OP 1004	430	-	-	-	-	-	-	-	-	-	-	-	-	-	-	-	430
OP 1005	569	-	21	-	-	-	-	-	-	-	-	-	-	-	-	-	569
OP 1006	-	4	4	-	50	337	17	-	357	261	-	-	-	564	342	-	564
OP 1007	-	9	4	-	63	354	35	-	417	326	-	6	-	781	503	-	781
OP 1008	-	-	1	-	-	207	13	-	143	144	-	4	-	381	136	-	381
OP 1009	-	-	1	-	-	233	10	-	244	174	-	6	-	479	246	-	479
OP 1010	-	-	-	-	-	-	12	-	-	-	-	171	63	-	-	-	171
OP 1011	-	-	-	-	-	-	21	-	-	-	-	197	75	-	13	-	197
OP 1012	-	-	-	-	-	-	144	-	-	455	-	389	466	-	-	-	466
OP 1013	-	-	-	-	-	-	170	-	-	728	-	440	512	-	-	-	728
OP 1014	-	104	-	-	-	529	243	-	-	9	1408	516	778	-	-	1277	1408
OP 1015	-	121	-	-	-	701	267	-	-	15	1487	571	872	-	87	1748	1748
OP 1016	-	1	-	-	-	248	-	-	-	2	1150	136	537	-	-	-	1150
OP 1017	-	3	-	-	-	273	-	-	-	-	1215	229	593	-	1	1236	1236
Route: 262 Ave	-	-	-	-	-	-	-	-	-	-	-	-	-	-	-	-	0
Route: 265th Ave	-	-	-	-	-	-	-	-	-	-	44	-	-	-	4	-	44
Route: 650th St	583	1356	-	-	255	596	567	10	54	895	2165	1223	1495	591	-	-	2165

Arrays 3-4 with 0 Degree Rest Angle Green Glare Min/Yr																	
Component	03a	03b	03c	03d	03e	03f	03g	03h	03i	03j	03k	03l	03m	04a	04b	04c	Maximum Minutes
OP 1006	-	-	-	-	-	-	-	-	-	-	-	-	-	1	211	-	211
OP 1007	-	-	-	-	-	-	-	-	-	-	-	-	-	1	211	-	211
OP 1008	-	-	-	-	-	-	-	-	-	-	-	-	-	-	88	-	88
OP 1009	-	-	-	-	-	-	-	-	-	-	-	-	-	-	88	-	88
OP 1010	-	-	56	-	-	-	-	-	-	-	-	-	-	-	-	-	56
OP 1011	-	-	58	-	-	-	-	-	-	-	-	-	-	-	-	-	58
OP 1012	-	-	-	-	-	117	-	-	-	-	-	-	-	-	-	-	117
OP 1013	-	-	156	-	-	206	-	-	-	-	-	-	-	-	-	-	206
Route: 262 Ave	-	-	-	-	-	-	-	-	-	-	-	-	-	-	-	-	0
Route: 650th St	-	-	-	266	711	600	-	-	543	-	-	-	-	84	278	-	711

Arrays 3-4 with 0 Degree Rest Angle Yellow Glare Min/Yr																	
Component	03a	03b	03c	03d	03e	03f	03g	03h	03i	03j	03k	03l	03m	04a	04b	04c	Maximum Minutes
OP 1006	-	-	-	-	-	-	-	-	-	-	-	-	-	1708	666	2787	2787
OP 1007	-	-	-	-	-	-	-	-	-	-	-	-	-	1780	703	2831	2831
OP 1008	-	-	-	-	-	-	-	-	-	-	-	-	-	1917	978	3096	3096
OP 1009	64	-	-	-	-	-	-	-	-	-	-	-	-	1998	1030	3164	3164
OP 1010	-	-	210	-	-	-	-	-	-	-	-	-	-	2396	926	2103	2396
OP 1011	-	1	272	-	-	-	-	-	-	-	-	-	-	2589	983	2163	2589
OP 1012	-	-	-	653	-	4	-	-	-	-	-	-	-	1649	-	-	1649
OP 1013	-	-	131	735	-	10	-	-	-	-	-	-	-	2154	-	-	2154
Route: 262 Ave	-	-	-	-	-	-	-	-	-	-	-	-	-	-	-	-	0
Route: 650th St	2034	-	-	1073	-	-	-	-	-	-	-	-	-	1565	940	3807	3807

[illegible]

Array 6 with 0 Degree Rest Angle Green Glare Min/Yr																			
Component	06a	06b	06c	06d	06e	06f	06g	06h	06i	06j	06k	06l	06m	06n	06o	06p	06q	06r	Maximum Minutes
OP 1018	-	-	167	631	-	-	629	-	276	-	-	-	552	-	96	-	-	-	631
OP 1019	-	-	172	639	7	-	642	-	293	-	-	-	562	-	101	-	-	-	642
OP 1020	-	-	100	594	-	-	674	-	311	-	-	-	723	-	356	-	32	-	723
OP 1021	-	-	104	597	3	-	698	-	322	-	-	-	731	-	366	-	40	-	731
OP 1022	-	-	-	-	-	-	-	-	-	-	-	-	-	-	-	-	-	-	0
OP 1023	-	-	-	-	-	-	-	-	-	-	-	-	-	-	-	-	-	-	0
OP 1024	-	-	-	112	-	87	593	-	249	-	-	-	867	-	537	-	261	54	867
OP 1025	-	-	-	113	-	91	604	-	331	-	-	-	905	-	552	-	288	61	905
OP 1026	537	-	262	172	78	1	90	144	75	-	-	-	425	-	1	-	-	-	537
OP 1027	551	-	282	161	116	147	98	229	75	-	183	-	426	-	294	-	-	-	551
OP 1028	-	-	-	-	-	-	-	-	-	91	-	-	-	-	-	-	-	-	91
OP 1029	-	-	-	-	-	-	-	-	-	92	-	-	-	-	-	-	102	130	130
OP 1030	-	-	-	-	-	-	-	-	-	199	-	-	-	-	-	-	-	-	199
OP 1031	-	-	-	-	-	-	-	-	-	198	-	-	-	-	-	-	11	-	198
OP 1032	-	-	-	-	-	-	-	-	-	386	-	-	-	-	-	-	-	-	386
OP 1033	-	-	-	-	-	-	-	-	-	396	-	-	-	-	-	20	-	-	396
Route: 660th St	-	-	139	476	-	-	538	-	202	-	-	-	267	-	-	-	-	-	538
Route: Co Rd 15 Segment 2	-	-	-	-	-	-	-	-	-	-	-	-	10	-	-	-	-	-	10
Route: Co Rd 6	-	-	367	-	765	-	-	-	131	730	335	-	-	-	-	15	-	-	765
Route: Co Rd 8	-	-	-	-	-	-	-	-	-	-	-	-	21	-	-	-	-	-	21

Array 6 with 0 Degree Rest Angle Yellow Glare Min/Yr																			
Component	06a	06b	06c	06d	06e	06f	06g	06h	06i	06j	06k	06l	06m	06n	06o	06p	06q	06r	Maximum Minutes
OP 1018	12	-	72	115	-	-	-	-	-	-	-	-	-	-	-	-	-	-	115
OP 1019	26	-	83	126	-	-	-	-	-	-	-	-	-	-	-	-	-	-	126
OP 1020	3	-	148	234	-	-	-	-	-	-	-	-	-	-	-	-	-	-	234
OP 1021	16	-	173	255	-	-	-	-	-	-	-	-	-	-	-	-	-	-	255
OP 1022	184	-	-	-	-	-	-	-	-	-	-	-	-	-	-	-	-	-	184
OP 1023	392	-	-	-	-	-	-	-	-	-	-	-	-	-	-	-	-	-	392
OP 1024	34	-	232	803	-	70	143	-	-	-	-	-	-	-	-	-	-	-	803
OP 1025	56	-	305	861	-	83	162	-	1	-	-	-	-	-	-	-	-	-	861
OP 1026	62	-	483	216	350	-	2125	2	1832	-	-	-	1123	-	7	-	-	-	2125
OP 1027	74	-	511	248	356	2	2446	4	2003	-	754	-	1207	-	157	-	-	-	2446
OP 1028	-	-	-	-	-	-	-	-	-	723	-	-	-	-	-	-	-	3	723
OP 1029	-	-	-	-	-	-	-	-	-	795	-	257	-	585	-	1408	21	34	1408
OP 1030	-	-	-	-	-	-	-	-	-	383	122	-	-	-	-	802	-	-	802
OP 1031	-	-	-	-	-	-	-	-	-	418	149	2	-	4	-	1066	494	1088	1088
OP 1032	-	-	-	-	-	-	-	-	-	56	-	-	-	-	-	-	-	-	56
OP 1033	-	-	-	-	-	-	-	-	-	65	-	-	-	-	-	697	-	-	697
Route: 660th St	9	-	51	105	-	-	-	-	-	-	-	-	-	-	-	-	-	-	105
Route: Co Rd 15 Segment 2	-	-	-	-	-	-	-	-	-	-	-	-	96	-	-	-	-	-	96
Route: Co Rd 6	-	-	-	-	-	-	-	-	14	827	586	-	-	-	-	566	-	-	827
Route: Co Rd 8	-	-	-	-	-	-	393	-	466	-	-	-	595	-	-	-	-	-	595

Appendix A
oDRA
Flight Path
Summary Glare
Data

[illegible][illegible]

Array 5 with 0 Degree Rest Angle Green Glare Min/Yr													
Component	05a	05b	05c	05d	05e	05f	05g	05h	05i	05j	05k	05l	Maximum Minutes
FP 1 TOB 340	-	-	-	-	-	-	-	-	-	-	-	-	0
FP 2 TOB 160	-	-	257	-	-	-	-	-	324	4	475	356	475
FP 3 TOB 220	-	-	-	-	-	-	-	-	-	-	-	-	0
FP 4 TOB 40	-	-	275	-	-	9	-	-	64	12	103	133	275
FP 5 RST 130	-	-	-	-	-	-	-	-	-	-	-	-	0
FP 6 RST 310	595	676	195	683	710	126	737	753	114	602	154	237	753
FP 7 RST 20	-	-	-	-	-	-	-	-	-	-	-	-	0
FP 8 RST 200	-	-	-	-	-	-	-	-	-	-	-	-	0
OP: 5000-ATCT	637	689	123	593	643	339	634	631	-	325	49	91	689

[illegible]

Appendix A
5 DRA
Flight Path and
ATCT
Summary Glare
Data

[illegible][illegible]

Appendix B

Detail Glare Data